BioChip J. (2013) 7(4): 367-374
DOI 10.1007/s13206-013-7408-0

Original Article

A microfluidic device for partial cell separation and deformability assessment

Diana Pinho[1,2], **Tomoko Yaginuma**[1] **& Rui Lima**[1,2]

Received: 3 September 2013 / Accepted: 27 October 2013 / Published online: 20 December 2013

Abstract Blood flow in microcirculation shows several interesting phenomena that can be used to develop microfluidic devices for blood separation and analysis in continuous flow. In this study we present a novel continuous microfluidic device for partial extraction of red blood cells (RBCs) and subsequent measurement of RBC deformability. For this purpose, we use polydimethylsiloxane (PDMS) microchannels having different constrictions (25%, 50% and 75%) to investigate their effect on the cell-free layer (CFL) thickness and separation efficiency. By using a combination of image analysis techniques we are able to automatically measure the CFL width before and after an artificial constriction. The results suggest that the CFL width increases with enhancement of the constriction and contributes to partial cell separation. The subsequent measurements of RBCs deformation index reveal that the degree of deformation depends on the constriction geometries and hematocrit after the cell separation module. The proposed microfluidic device can be easily transformed into a simple, inexpensive and convenient clinical tool able to perform both RBC separation and deformability analysis in one single device. This would eliminate the need for external sample handling and thus reducing associated labor costs and potential human errors.

Keywords: Biomicrofluidics, Microfluidic devices, Microcirculation, Blood on chips, Red blood cells, Cell separation, Cell deformability, Deformation index

[1]Polytechnic Institute of Bragança, ESTiG/IPB, C. Sta. Apolonia, 5301-857 Bragança, Portugal
[2]CEFT, Faculdade de Engenharia da Universidade do Porto (FEUP), R. Dr. Roberto Frias, 4200-465 Porto, Portugal
Correspondence and requests for materials should be addressed to R. Lima (✉ruimec@ipb.pt)

Introduction

Cell separation and identification are essential in a variety of biomedical applications including cell biology, diagnostic and therapeutic methods. Blood is a non-Newtonian fluid containing extremely rich amount of information about the physiological and pathological state of the human body. However, due to its complexity there are few accurate analysis methods. Most of the standard techniques used cell separation and sorting are often labor intensive or require additional external labels to identify cells.

Blood flow in microcirculation shows several interesting phenomena that can be used to develop microfluidic devices for blood separation and analysis in continuous flow. These phenomena include plasma skimming[1], cell-free layer (CFL)[2-4], leukocyte margination[5] and bifurcation law[6]. Recently, several researchers have used these effects and replicated in microfluidic systems. In microchannels RBCs, due to their deformability and lift forces, tend to be concentrated around the center of the microchannels while white blood cells (WBCs) and rigid RBCs (such as Malaria RBCs) tend to migrate to the CFL originated at regions close to the walls[1-5]. Bifurcation law[6] states that RBCs behavior, in microchannels with bifurcations, tends to be oriented to the wide microchannel. A number of microfluidic devices have been developed to take advantage of these natural hemodynamics phenomena. Shevkoplyas *et al.*[7] developed a microdevice to isolate WBCs from a blood sample by using the margination effect, whereas Hou *et al.*[8] have very recently proposed a biomimetic separation device to separate normal RBCs from malaria infected RBCs. Other researchers have found several advantages to control and manipulate blood flow in microfluidic devices. Fujiwara *et*

al.[9] have found evidence that it is possible to create an artificial CFL under appropriate hemodynamic and geometrical conditions, and also the CFL thickness is strongly influenced by the RBC deformability. Recently, Ishikawa *et al*.[10] and Leble *et al*.[11] have shown the existence of thin CFL in the centre of the microchannel, just downstream of a confluence. This phenomenon is due to the existence of a CFL in both inner walls and a consequent formation of a triangular CFL in the region of the confluence apex[10,11]. Faivre *et al*.[12] and Sollier *et al*.[13] have demonstrated that the CFL could be enhanced by using a microchannel containing a constriction followed by sudden expansion to separate plasma from the whole *in vitro* blood. However, most of these studies aim at the complete extraction of cells from plasma, which is not the case of the present study.

The main objective of the proposed microfluidic device is to separate certain amount of RBCs from plasma and then measure the deformability of individual RBCs downstream in one single step. RBC deformability is important in a clinical sense as it is related to several diseases such as diabetes, malaria, as well as cardiovascular disorders[14]. These diseases are at times fatal and early detection is crucially preferable. In this sense, RBC deformability can be a new biomarker and the fast and easy measurement methods are required. Former studies on RBC deformability have introduced some methodologies such as micropipette aspiration and optical tweezers where basically RBCs are stretched and the pressure or force for their extension is measured[15,16]. Whilst these studies have revealed useful RBCs mechanical properties, these methods reqire large amount of preparation and are very time consuming. For fast analysis of vast amount of blood samples, these traditional measurement methods are unlikely to be appropriate. Moreover, since the preceded cell separation process is needed, the microfluidic devices which are easy to manipulate their microchannel geometries are more suitable for our purposes. A typical microdevice for RBC deformation studies uses a microchannel having a shape of sudden constriction in order to elongate cells. Zhao *et al*.[17] used a straight microchannel with a sudden narrowing and expanding constriction. Lee *et al*.[18], Yaginuma *et al*.[19-20], and Faustino *et al*.[21], on the other hand, used microchannels with a hyperbolic shape contraction followed by a sudden expansion region. These microfluidic experiments showed high deformability of RBCs when travelling through a contraction region. However, those studies did not include the preceded cell separation process as they have solely performed deformability measurements after an additional sample preparation[19-21].

The proposed microfluidic device aims to obtain a CFL with a low enough RBC concentration to perform cell deformability measurements downstream the separation constriction. This study is divided in two main parts. Firstly, a simple microfluidic device with different constrictions (25%, 50% and 75%) is used to test the RBCs separation. Secondly, a more complex device, able to perform in a single step both RBC separation and deformability analysis, was tested. This first tentative to integrate in one single device both tasks of separation and deformation have shown not only the viability of this new clinical strategy but also new findings that will be crucial to optimize the design for this kind of microfluidic device.

Results

CS microfluidic device: constriction effect in the CFL thickness

In the CS device we have evaluated the effect of the constriction on the CFL thickness and consequently on the separation effectiveness. This study was performed with different r_C (0.25, 0.5 and 0.75), at a Hct of 9% and with three different flow rates (1 μL/min, 5 μL/min and 10 μL/min).

Qualitative flow visualization results show that all constrictions enhance CFL thickness. Furthermore, it is clear that the enhancement is more pronounced for the microchannel with r_C=0.25. To obtain more detail results about the constriction effect, quantitative mea-

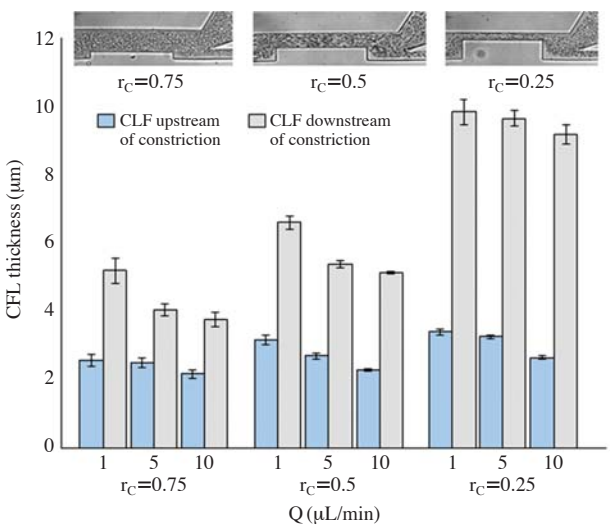

Figure 1. CFL thickness for both upstream (CFL_u) and downstream (CFL_d) constrictions at different flow rates (1 μL/min, 5 μL/min and 10 μL/min) and different constriction ratios (r_C=0.25, r_C=0.5 and r_C=0.75).

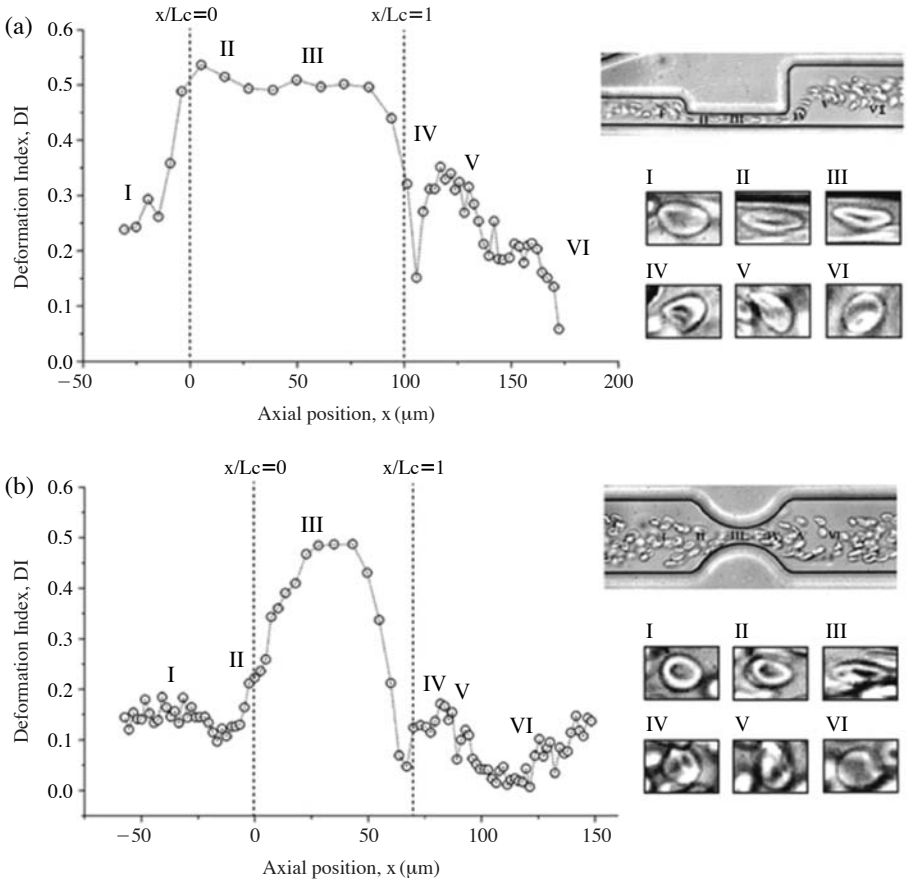

Figure 2. DI values of a single RBC flowing through (a) a sudden contraction and (b) a smooth contraction.

surements of the CFL thickness were taken both upstream (CFL_u) and downstream (CFL_d) the constrictions at different flow rates (see Figure 1).

Overall the quantitative measurements of the CFL thickness, presented in Figure 1, show clearly that all the constrictions tested enhance the CFL thickness at downstream region (CFL_d). It is also clear that the CFL_d increases with decreasing r_C and this enhancement is more pronounced for r_C=0.25 where CFL_d is about three orders of magnitude greater than the CFL_u. Additionally, these results show a tendency of the CFL thickness to decrease with increasing flow rate, which corroborates the results obtained using a microchannel with similar constrictions and a Hct of 2.6%[12]. Note that, this tendency is more pronounced for r_C= 0.5 and 0.75.

CSD microfluidic device: constriction effect and deformation measurements

Downstream the CS region, RBC deformation measurement region is followed in the same microchannel as shown in Figure 7 in supplementary materials. In this study, two geometrically different constriction regions, one with a sudden contraction and another with a smooth contraction, were tested in order to examine efficient deformability measurements. For this examination, the upstream constriction (CS region) with r_C=0.5, an inlet Hct of 9%, and a flow rate of 1 μL/min was used.

The Hct at this region should be around 2.4% and RBCs tend to flow in line and the majority of them start becoming like a parachute or umbrella shape when they pass through a sudden constriction microchannel with a width of 7 μm. This RBC deformation behaviour is mainly due to the constriction to be smaller of the normal size of human RBC (8 μm) and to the shear flow. Figure 2a shows the x-axial DI values of one individual RBC flowing through the sudden constriction microchannel. At the contraction entrance (x/Lc=0), the highest DI was obtained due to a strong shear stress caused by the sudden narrowing of the flow field. Then the RBC starts changing their shape from an ellipsoid to a parachute, reaching a low DI

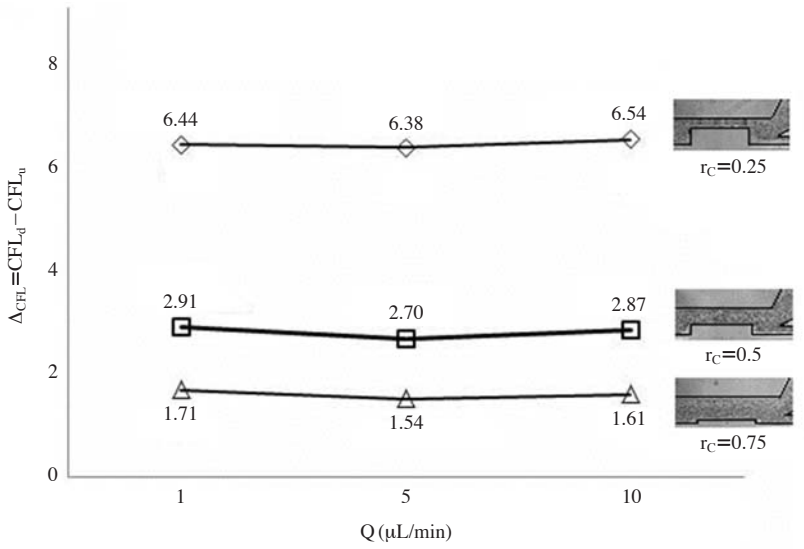

Figure 3. The difference of the CFL upstream and downstream of the constriction (Δ_{CFL}) at different flow rates and different constriction ratios (r_C=0.25, r_C=0.5 and r_C=0.75).

value at the exit of the contraction (x/Lc=1, see also the image IV in Figure 2a.) The sudden contraction is effective to observe a strong deformation of RBCs with high shear stress. However, proceeded DI values are slightly unreliable as parachute shapes are rather variable and the definition of major and minor axis of the cell in this shape does not have the same meaning for the ellipsoid shape. Besides this, overlaps of the cells were often observed, which is not ideal for deformation measurements especially when an automatic method is applied. The Hct control has to be carefully done in the upper stream.

Figure 2b shows the DI values of one single RBC flowing through the smooth contraction region for deformability measurement. It is clear that the highest DI is observed around x/Lc=0.5. In this type of constriction, in the middle of the microchannel (y=0 and z=0) extensional force is likely to be more dominant over shear force, where RBCs tend to flow stably with no rotation or orientation. For good image analysis results it is important to measure RBCs flowing in the same orientation so that this condition is ideal.

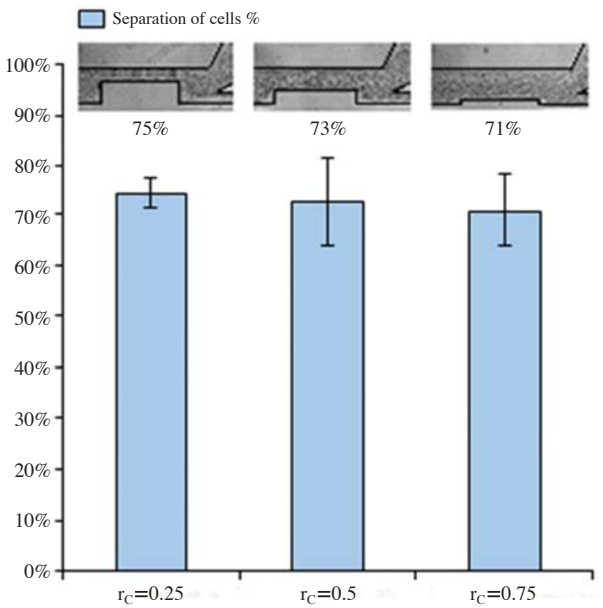

Figure 4. Separation rate of the RBCs flowing to the outlet region number 2 (upper side outlet). The measured values are expressed as the mean±standard deviation according to a t-test analysis at a 95% confidence interval.

Discussion

To analyse in more detail the effect of the artificial constrictions on the CFL thickness, Figure 3 shows the Δ_{CFL} for each constriction as a function of the flow rate. These results show clearly that Δ_{CFL} increases with decreasing the r_C and this enhancement is more pronounced for r_C=0.25 where Δ_{CFL} is about two to four orders of magnitude greater than Δ_{CFL} for r_C=0.5 and r_C=0.75, respectively. It is worth mentioning that the highest Δ_{CFL} corresponds to r_C=0.25 and is independent of the flow rate. For r_C=0.5 and r_C=0.25 for low flow rate there is a tendency to decrease but tend to flattened to higher flow rates. However these results

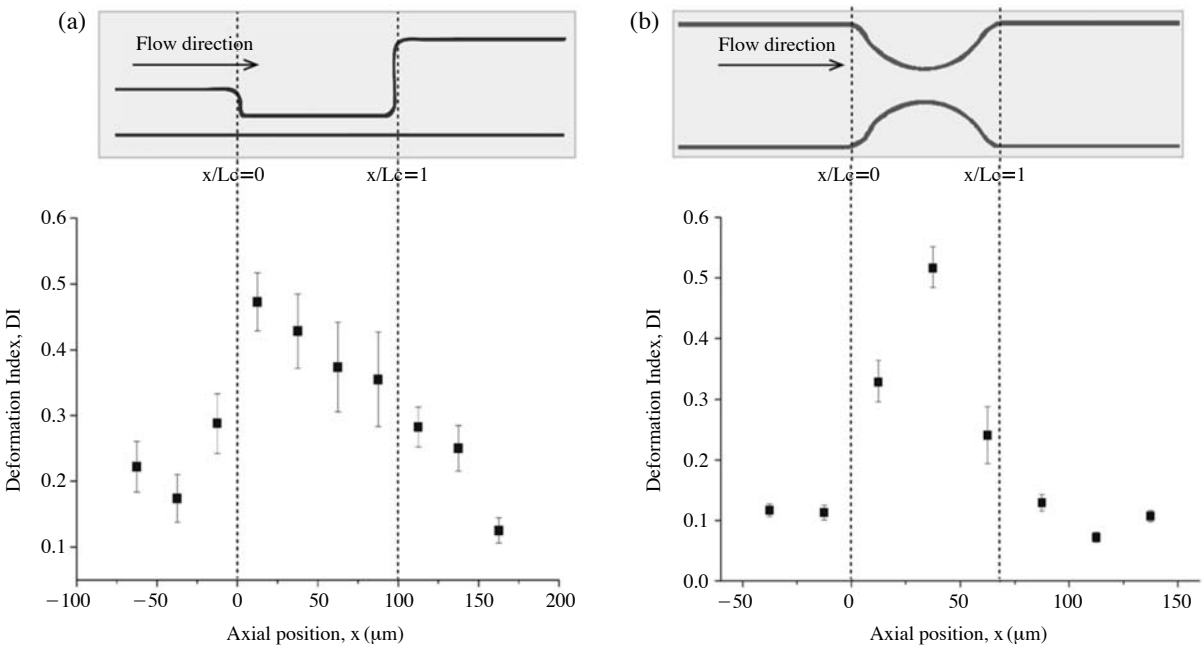

Figure 5. Mean DI values of two deformation measurement modules: (a) a sudden and (b) a smooth contractions.

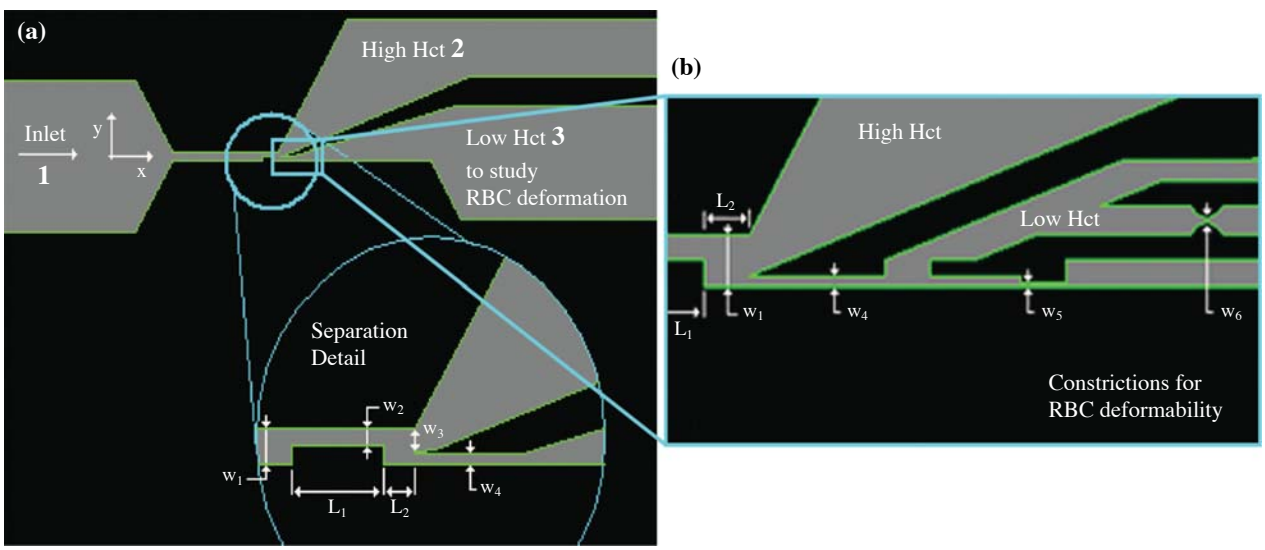

Figure 6. Schematic drawing of the microfluidic device. (a) the entire view and close-up view of cell separation part. The dimensions of L_1, L_2, w_1, w_3, w_4, are 300 μm, 100 μm, 100 μm, 80 μm and 20 μm, respectively. The different constrictions were used (w_2=75 μm, 50 μm and 25 μm). (b) the view of deformation measurement part. The dimensions of w_5 and w_6 are 7 μm and 10 μm, respectively. The height of the microchannel is 51 μm.

show evidence that the constriction has a strong impact in the CFL thickness (see Figure 4).

Figure 4 shows the separation rate of cells flowing to the outlet region number 2 (see Figure 6), i. e., for r_C=0.5 this constriction can efficiently separate about 73% of blood cells to region 2 and remaining 27% of cells to the deformation region. This separation estimation is based on the same image analysis approach used to calculate the CFL thickness. Briefly, we have used binary images and considered that all the white part, upstream the constriction, corresponds to a uniform distribution of the RBCs core to be 100%. Hence,

by measuring the CFL thickness downstream the constriction we were able to estimate the separation rate depending on the size of the constriction. As expected, the constriction with higher efficiency was the one with r_C=0.25. Although statistical analysis have shown a significant difference between r_C=0.25 and r_C=0.75, this is not the case for r_C=0.5. Hence, we believe that the most effective way to get a considerable difference between r_C=0.25 and r_C=0.5 is by decreasing the geometrical parameter L_2 (see Figure 6). In the present study we have decided to use the constriction with r_C=0.5 to test the ability of the proposed device to perform in one single step both separation and deformation of blood cells. Note that for r_C=0.5 and by considering a feed Hct to be about 9%, the local Hct in the outlet 3 (deformation region) is around 2.4%. Very recently, by using 1% Hct we have successfully measured the RBC deformability in hyperbolic contractions[20]. In order to achieve 1% Hct with the proposed microfluidic device the separation rate should be around 90% and consequently r_C must be less than 0.25. Alternatively, by decreasing the geometrical parameter L_2, to a dimension less than 100 μm, it will be possible to achieve easily local Hcts less than 1%.

In terms of the deformation measurements, Figure 5 shows average DI values of ten RBCs flowing through the two different constriction regions. The maximum DI value is in both cases relatively the same, however, for the sudden contraction case (a) the maximum DI is located close to the constriction entrance whereas for the smooth case (b) the maximum DI is located around the middle of the constriction. In addition, in the constricted region in (a) RBCs tend to flow as parachute like shape and the DI values are not truly comparative in the sequence of cell behaviour throughout the deformation analysis region of the device. At least, the region for measurements has to be carefully selected for a meaningful comparison. On the other hand, the smooth contraction provides less deviation of DI results and indicates clearly an appropriate measurement region (x/Lc=0.5), i. e., middle of constriction. The majority of the cells are flowing with the same orientation at the centreline of the channel where the cells are under an extensional flow dominated regime and as a result they tend to elongate in y direction induced mainly by this extensional force. This stable state of the RBCs makes this geometry suitable to measure small changes of RBC deformability. More detailed studies on RBCs extensional flow effects can be found elsewhere[19-21].

As mentioned before, by using a constriction with r_C=0.5, we have observed collisions and the overlap of neighbouring cells flowing within the measurement region. In the CS region, the Hct of the flowing fluid is reduced from 9% to ≈2.4% but ideally it needs to be less than that. Nevertheless, it is worth mentioning that by reducing Hct to less than 2% the number of RBCs to measure may not be large enough to obtain a significant statistical picture of the results. Therefore, an optimization of channel, i.e. change in depth, needs to be done in order to obtain the best representative results of the RBCs DI.

Conclusions

The conventional microfluidic methods for measuring RBC deformability are often labor intensive and require additional sample modification and preparation. In this paper, we present a new, simple microfluidic device able to perform both RBCs separation and deformability assessment in one single step. In general, our results indicate that the proposed device can perform both operations (separation and deformation) successfully. The reported results show evidence that the constriction has a strong impact on the CFL thickness and consequently on separation rate. Moreover, the deformability results show clearly that most appropriate geometry to measure RBC deformability is the microchannel containing a smooth constriction region. In this kind of geometry due to the existence of a dominant extensional force the majority of the RBCs tend to flow with the same orientation. This stable performance of the RBCs may prove to be enough sensitive to detect small changes of RBC deformability and thus it may have the ability to diagnose early stage RBC related diseases such as diabetes, malaria and sickle cell anemia. Therefore, the integrated and simple continuous system operations make the proposed microfluidic device a potential diagnostic technique to be applied to both healthy cells and blood cell diseases.

Materials and Methods

Working fluids

The working fluid used in this study was dextran 40 (Dx40) containing about 9% (i.e. Hematocrit, Hct=9) by volume of human RBCs. More details can be found in supplementary Materials.

Microdevice geometries

The microfluidic devices tested in this study were fabricated using a soft lithography technique and consist of two main parts: a cell separation region and a cell deformation region. The microchannel height was measured by a profilometer to be 51 μm.

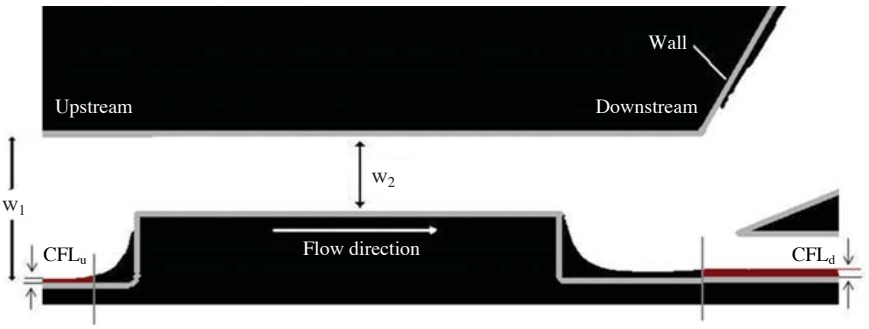

Figure 7. Schematic view of the contraction-expansion geometry, identifying the relevant variables.

Fabrication of the microfluidic devices

The polydimethylsiloxane (PDMS) rectangular microchannels were fabricated using a soft lithographic technique. A detailed description of the fabrication process can be found elsewhere[22,23]. Briefly, the microchannel geometry was drawn using Autocad, and a high resolution photomask was manufactured. The solid master was then fabricated on a silicon wafer with an ultra-thick photoresist (SU-8 50; Kayaku MicroChem, Japan). The PDMS prepolymer was prepared by mixing a comercial prepolymer and catalyzer (Silpot 184; Dow Corning, USA) at a weight ratio of 10 : 1. After the mixture was degassed under vacuum, the PDMS was poured into the SU-8 photo-resist master mold and cured by baking for about 2 h at 70˚C. Both master and PDMS were cooled to room temperature and the PDMS was peeled from the master. The input/output ports are made by means of micro-pipette tips. Finally, the PDMS was washed with ethanol and brought into contact with a clean slide glass, where a reversible seal formed spontaneously.

Cell separation (CS) microfluidic device

To study the effect of a single constriction on the cell separation, a simple microfluidic device with different constriction sizes was developed. This first device had only a separation region that consists of a straight microchannel with 100 μm wide (w_1) with different constriction regions of 75 μm, 50 μm and 25 μm wide (w_2). Figure 6a shows the microfluidic device with the different contractions used to test the RBCs separation.

Cell separation and deformation (CSD) microfluidic device

To investigate the ability to perform in a single step both RBC separation and deformability analysis, a microfluidic device having a cell separation region followed by an outlet cell deformation region was tested. Note that this latter region has a concentration of cells lower than the feed Hct. This tested device had feed microchannel of 100 μm (w_1), a constriction of 50% (w_2=50 μm) followed by different kind of constrictions to perform RBC deformability. More detailed information about the dimensions can be seen in Figure 7 in supplementary materials.

Experimental set-up

In this study we have used a high-speed video microscopy system. The details of the experimental system and the image analysis procedure are explained in supplementary materials.

Contraction ratio, CFL thickness and deformation index (DI)

In this study we used microchannels with the width (w_1) of the feed channel of 100 μm and the width (w_2) of the constrictions varying from 25 μm, 50 μm, up to 75 μm. To examine the effect of these three different artificial constrictions (25%, 50% and 75%) on the CFL thickness, the contraction ratio (r_C) was defined as follows:

$$r_C = \frac{w_2}{w_1} \quad (1)$$

Note that, the r_C of the constrictions 25 μm, 50 μm and 75 μm corresponds to 0.25, 0.5 and 0.75, respectively.

To analyze the CFL thickness, measurements were taken upstream and downstream the artificial constrictions, as show in Figure 7. CFL_u corresponds to the thickness of the CFL upstream the constriction, and the CFL_d to the thickness downstream the constriction. The difference of the CFL upstream and downstream of the constriction was given by:

$$\Delta_{CFL} = CFL_d - CFL_u \quad (2)$$

For characterizing deformability of RBCs, we use deformation index (DI) which is defined as follows.

$$DI=\frac{(L_{major}-L_{minor})}{(L_{major}+L_{minor})} \quad (3)$$

Note that L_{major} and L_{minor} are the major and minor axis lengths of the RBC. We also calculated the length error which might be caused by the camera's exposure time but the values were sufficiently low ($\ll 1$ μm) throughout the measured regions so that these possible deviation was ignored.

Acknowledgements The authors acknowledge the financial support provided by 2007 Global COE Program "Global Nano-Biomedical Engineering Education and Research Network", Japan and Grant-in-Aid for Science and Technology PTDC/SAU-BEB/108728/2008, PTDC/SAU-BEB/105650/2008, PTDC/EME-MFE/099109/2008, PTDC/SAU-ENB/116929/2010 and scholarship SFRH/BD/89077 /2012 from FCT (Science and Technology Foundation), COMPETE, QREN and European Union (FEDER). The authors are also very grateful to Dr. Mónica Oliveira (Strathclyde University), Professor Takuji Ishikawa and Professor Takami Yamaguchi (Tohoku University) for their suggestions and support to this research work.

References

1. Caro, C., Pedley, T., Schroter, R. & Seed, W. The Mechanics of the Circulation. Oxford University Press, 1978.
2. Lima, R. *et al*. Measurement of individual red blood cell motions under high hematocrit conditions using a confocal micro-PTV system. *Ann. Biomed. Eng*. **37**, 1546-1559 (2009).
3. Fujiwara, H. *et al*. Red blood cell motions in high-hematocrit blood flowing through a stenosed microchannel. *J. Biomech*. **42**, 838-843 (2009).
4. Lima, R. *et al*. Axisymmetric polydimethysiloxane microchannels for in vitro hemodynamic studies. *Biofabrication* **1**, 1-7 (2009).
5. Goldsmith, H. & Spain, S. Margination of leukocytes in blood flow through small tubes. *Microvasc. Res*. **27**, 204-222 (1984).
6. Yang, S., Undar, A. & Zahn, J.D. A microfluidic device for continuous, real time blood plasma separation. *Lab Chip* **6**, 871 (2006).
7. Shevkoplyas, S.S., Yoshida, T., Munn, L.L. & Bitensky, M.W. Biomimetic Autoseparation of Leukocytes from Whole Blood in a Microfluidic Device. *Anal. Chem*. **77**, 933-937 (2005).
8. Hou, H.W. *et al*. Deformability based cell margination - A simple microfluidic design for malaria-infected erythrocyte separation. *Lab Chip* **10**, 2605-2613 (2010).
9. Fujiwara, H. *et al*. Red blood cell motions in high-hematocrit blood flowing through a stenosed microchannel. *J. Biomech*. **42**, 838-843 (2009).
10. Ishikawa, T. *et al*. Asymmetry of blood flow and cancer cell adhesion in a microchannel with symmetric bifurcation and confluence. *Biomed. Microdevices* **13**, 159 (2011).
11. Leble, V. *et al*. Asymmetry of red blood cell motions in a microchannel with a diverging and converging bifurcation. *Biomicrofluidics* **5**, 044120 (2011).
12. Faivre, M., Abkarian, M., Bickraj, K. & Stone, H. Geometrical focusing of cells in a microfluidic device: an approach to separate blood plasma. *Biorheology* **43**, 147-159 (2006).
13. Sollier, E., Cubizolles, M., Fouillet, Y. & Achard, J. Fast and continuous plasma extraction from whole human blood based on expanding cell-free layer devices. *Biomed. Microdevices* **12**, 485-497 (2010).
14. Mokken, F.C., Kedaria, M., Henny, C.P., Hardeman, M.R. & Gelb, A.W. The clinical importance of erythrocyte deformability, a hemorrheological parameter. *Ann. Hematol*. **64**, 113-122 (1992).
15. Musielak, M. Red blood cell deformability measurement: Review of techniques. *Clin. Hemorheol. Micro*. **42**, 47-64 (2009).
16. Shiga, T., Maeda, N. & Kon, K. Erythrocyte rheology. *Crit. Rev. Oncol. Hemat*. **10**, 9-48 (1990).
17. Zhao, R. *et al*. Microscopic investigation of erythrocyte deformation dynamics. *Biorheology* **43**, 747-765 (2006).
18. Lee, S.S., Yim, Y., Ahn, K.H. & Lee, S.J. Extensional flow-based assessment of red blood cell deformability using hyperbolic converging microchannel. *Biomed. Microdevices*. **11**, 1021-1027 (2009).
19. Yaginuma, T., Oliveira, M.S.N., Lima, R., Ishikawa, T. & Yamaguchi, T. Red blood cell deformation in flows through a PDMS hyperbolic microchannel. *Proceedings of NSTI-Nanotech* **2**, 505-507 (2011).
20. Yaginuma, T., Oliveira, M.S.N., Lima, R., Ishikawa, T. & Yamaguchi, T. Human red blood cell behavior under homogeneous extensional flow in a hyperbolic-shaped microchannel. *Biomicrofluidics* **7**, 054110 (2013).
21. Faustino, V. *et al*. Flow of red blood cells suspensions through hyperbolic microcontractions. Visualization and simulation of complex flows in biomedical engineering. In: Lima, R., Ishikawa, T., Imai, Y. & Oliveira, M.S.N. (Eds), Springer, 2013 (in press).
22. Lima, R. *et al*. *In vitro* blood flow in a rectangular PDMS microchannel: experimental observations using a confocal micro-PIV system. *Biomedical Microdevices* **10**, 153-167 (2008).
23. Lima, R. *et al*. Microscale flow dynamics of red blood cells in microchannels: an experimental and numerical analysis. In: Tavares and Jorge (Eds) Computational Vision and Medical Image Processing: Recent Trends, Springer 19, 297-309 (2011).